

Possibility of H dibaryon production with energetic hyperon and meson beams

Murray A. Moinester*

*School of Physics and Astronomy, Raymond and Beverly Sackler Faculty of Exact Sciences,
Tel Aviv University, 69978 Ramat Aviv, Israel*

Carl B. Dover[†]

Department of Physics, Brookhaven National Laboratory, Upton, New York 11973

Harry J. Lipkin[‡]

*Department of Nuclear Physics, Weizmann Institute of Science, Rehovot 76100, Israel
and School of Physics and Astronomy, Raymond and Beverly Sackler Faculty of Exact Sciences,
Tel Aviv University, 69978 Ramat Aviv, Israel*

(Received 13 May 1992)

We present cross section estimates and describe possible experiments for the production of the doubly strange six quark H dibaryon in the two-body reactions $\Xi^- + p \rightarrow \pi^0 + H, \rho^0 + H$, $\Sigma^- + p \rightarrow K^0 + H, K^{0*} + H$, and $\Lambda + p \rightarrow K^+ + H, K^{*+} + H$, in the energy region from 1 to 20 GeV. We also consider the semi-inclusive process $\Xi^- + p \rightarrow H + \bar{p} + X$ in the region of a few hundred GeV/c, and two step processes induced by pion and kaon beams in the 2–6 GeV/c range.

PACS number(s): 25.80.Nv, 25.80.Pw, 14.20.Pt

I. INTRODUCTION

There is considerable theoretical and experimental interest in searches for dibaryon resonances or bound states (other than the deuteron). A particularly attractive candidate for such a bound state is the double-strange H dibaryon proposed by Jaffe [1]. The H has a quark structure $uuddss$, coupled to spin-parity $J^\pi=0^+$ and isospin $I=0$. There are numerous theoretical estimates of the H mass in the MIT bag model [1–3], the constituent quark model [4], potential models [5], the Skyrmin picture [6–8], the hybrid quark-cluster model [9,10], the color-dielectric model [11], instanton models [12], and lattice quantum chromodynamics (QCD) [13,14]. The predicted H masses m_H vary significantly from $m_H \simeq 2m_n$ (Ref. [13]) to values above the strong decay $\Lambda\Lambda$ threshold (Ref. [12]). Jaffe's original result that the H is bound by an attractive short-range color-magnetic interaction between quark pairs has been challenged by calculations showing a drastic reduction of the attraction by SU(3)-flavor symmetry breaking [3–5].

In view of the large uncertainties in the predictions of m_H , several complementary experiments are necessary in order to achieve sensitivity to a broad range of m_H and lifetime τ_H . A model calculation of τ_H was done by Donoghue *et al.* [15], assuming that the H is an SU(3)

singlet. This is reasonable for sufficiently strong binding. In the mass range $2134 < m_H < 2231$ MeV/c², the weak decay process $H \rightarrow \Sigma^- p$ figures prominently. In our later considerations, this mode will represent one of the possible experimental signatures.

In the absence of reliable detailed calculations, we present some general physical features common to many models which can serve as a guide to further investigations. In meson-exchange models, the longer-range part of the $\Lambda\Lambda \rightarrow \Lambda\Lambda$ potential is attractive [16], whereas the short-range part due to quark-gluon exchange is repulsive [17]. At short range, the $\Lambda\Lambda$, $\Sigma\Sigma$, and ΞN channels are strongly coupled, i.e., off-diagonal matrix elements are comparable to those for the diagonal $\Lambda\Lambda \rightarrow \Lambda\Lambda$ transition. This strong channel coupling is responsible for generating the H . The repulsive short-range diagonal $\Lambda\Lambda$ interaction raises two very interesting possibilities. (1) Unbound metastable dibaryons may exist with an energy below the potential barrier created by the repulsive interaction. Such states would appear as narrow low-energy $\Lambda\Lambda$ resonances with a width determined by the barrier penetration factor. (2) Doubly-strange $\Lambda\Lambda$ hypernuclei may exist, even though the H also exists at a stable bound state. Two Λ 's bound in the lowest s orbit of a hypernucleus may be kept apart by a repulsive short-range potential barrier long enough to allow weak decay to compete with H formation. This would not prevent H formation in a hadronic experiment with an energy above the barrier or in another channel; e.g., $\Xi^- p$, which would have a very different short-range interaction.

Estimates of cross sections for H production are difficult because of the uncertainty in the underlying dynamics, in particular the probability of fusion of two baryons to form an H . Here, we attempt estimates based on the analogous process of deuteron production by

*Electronic address: MURRAY@TAUPHY.TAU.AC.IL (internet)

[†]Electronic address: DOVER@BNLDAG (bitnet)

[‡]Electronic address: FTLLIPKIN@WEIZMANN.WEIZMANN.AC.IL (internet)

nucleon-nucleon fusion, with the caveat that the fusion processes in deuteron and H production could be completely different.

The nucleon-nucleon interaction is known experimentally to have a repulsive core and an intermediate-range attraction. The deuteron wave function is described to a good approximation as a state of two nucleons, kept apart by the short-range repulsion and without excitation of the quark degrees of freedom. The strangeness $S = -2$ interactions are poorly known experimentally, but models that bind the H with a color-magnetic interaction produce an H wave function with a six-quark core at short distances that is very different from the deuteron.

If the H is weakly bound, it can have a $\Lambda\Lambda$ tail extending out beyond the range of interaction, analogous to the large nucleon-nucleon tail of the deuteron. The size and range of the tail depends upon the binding energy and on whether there is indeed a repulsive potential barrier from a quark-exchange force, which would confine the quarks and reduce the tail. A weakly bound H , analogous to the deuteron, might also be produced by conventional meson-exchange forces [18].

The probability for two baryons to fuse into an H depends upon the overlap of the two-baryon wave function with the H wave function. This in turn depends upon the relative contributions of the $\Lambda\Lambda$ tail and the six-quark core with a structure envisioned by Jaffe [1] as having total space symmetry and the flavor structure of the SU(3)-singlet combination of $\Lambda\Lambda$, $\Sigma\Sigma$, and ΞN baryon-baryon channels. The fusion overlap could be very different from the case of the deuteron, where there are two well-defined nucleons and the division of the six quarks into three-quark color-singlet clusters is well determined. We do not attempt to solve the dynamical problem of baryon-baryon fusion, and instead use some simple spin and flavor factors in comparing the deuteron and H cases. We also neglect the effects of "hidden color," which arise as a consequence of the antisymmetrization of the six-quark wave function.

A variety of experimental searches for the H dibaryon are in progress or under discussion. A candidate event for the H has been reported by Shahbazian *et al.* [19], based on the study of high-energy proton interactions in propane. Two experiments [20,21] are underway at the Brookhaven Alternating Gradient Synchrotron (AGS) which apply the (K^-, K^+) double-strangeness exchange process. In one experiment, the $K^- + p \rightarrow K^+ + \Xi^-$ reaction is used to produce a tagged Ξ^- , which subsequently engages in the $\Xi^- + d \rightarrow n + H$ reaction in a deuterium target. The two-body nature of this process is an important advantage, since one does not need to detect the H . The predicted [22] branching ratio for $\Xi^- + d \rightarrow n + H$ decreases swiftly with decreasing m_H , however, so one is not sensitive to a deeply bound H . In the second AGS experiment, the H is produced in the reaction $K^- + {}^3\text{He} \rightarrow K^+ + H + n$. Here we are sensitive to a broad range of m_H , but a $K^+ - n$ coincidence measurement is needed in order to reconstruct the invariant mass of the H . It is possible to produce the H in \bar{p} -nucleus interactions, for instance, $\bar{p} + {}^3\text{He} \rightarrow (KK\pi)^+ + H$, as discussed by Kilian [23], but the branching ratio is very small since

two strange-quark pairs ($s\bar{s}$) must be generated in the final state. Finally, we mention the possibility of creating the H in relativistic heavy-ion collisions. Rather copious H formation rates have been estimated in the coalescence model [24,25]. In view of the large multiplicity of pions produced in such encounters, one must detect the H directly by its $H \rightarrow \Sigma^- p$ decay, by $Hp \rightarrow \Lambda\Lambda p$ diffractive dissociation, or by time-of-flight and calorimetry methods, as in AGS experiment [26] E864. To be discovered with the latter technique, τ_H must be longer than a few tens of nanoseconds.

In the present paper, we investigate the viability of an approach to H production using high-energy hyperon beams ($\Sigma^-, \Xi^-,$ or Λ) or meson beams (π^\pm, K^-). We used tagged Ξ^- 's from the $K^- p \rightarrow \Xi^- K^+$ reaction, Σ^- 's from the $K^- p \rightarrow \Sigma^- \pi^+$ or $\pi^- p \rightarrow \Sigma^- K^+$ reaction, or Λ 's from the $K^- p \rightarrow \Lambda p$ or $\pi^- p \rightarrow \Lambda K^{0*}$ reaction. We then consider two-body reactions induced by hyperons, such as

$$\begin{aligned} \Sigma^- p &\rightarrow H + (K^0, K^{0*}), \\ \Xi^- + p &\rightarrow H + (\pi^0, \rho^0), \\ \Lambda + p &\rightarrow H + (K^+, K^{*+}). \end{aligned} \quad (1.1)$$

We consider here only channels involving pseudoscalar or vector mesons, although we expect comparable cross sections for production of the $f_2(1270)$, which decays 85% of the time to the $\pi^+\pi^-$ channel. Similarly, in addition to $K^*(892)$, which has a 100% decay to $K\pi$, we expect to also produce $K_2^*(1430)$, which has a 50% decay to $K\pi$. We also consider inclusive or semi-inclusive production ($\Sigma^- + p, \Xi^- + p \rightarrow H + X$, or $H + \bar{p} + X$). We do not attempt to predict absolute cross sections, but rather the ratios to the corresponding deuteron-production reactions

$$p + p \rightarrow d + \pi^+, \quad (1.2a)$$

$$p + p \rightarrow d + \rho^+, \quad (1.2b)$$

$$p + p \rightarrow d + X. \quad (1.2c)$$

Based on measurements of the deuteron cross sections in the region of laboratory momentum between 4 and 20 GeV/c, we conclude that studies of some of the reactions (1.1) may be experimentally feasible at these energies. At higher c.m. energy \sqrt{s} , the two-body cross sections drop rapidly ($\sim s^{-3}$), and one must rely on inclusive or semi-inclusive processes. At CERN Super Proton Synchrotron or Fermilab energies, the two-body cross sections for H production will be unmeasurably small.

The use of hyperon beams for H production has certain advantages. For instance, the Ξ^- brings in the required two units of strangeness, so one does not suffer the penalty factor associated with the creation of additional $s\bar{s}$ pairs (of course, this penalty is already reflected in the modest intensity of Ξ^- beams). At high energies, the produced particles and the decay fragments from the H are all focused in a forward cone in the laboratory system, so one has a reasonable efficiency for detecting all particles in the final state. In the case of the two-body reactions (1.1), without detecting the H decay products, we

have clearly identifiable final states with only charged particles in some cases, namely,

$$HK, H\rho^0 \rightarrow \Sigma^- p \pi^+ \pi^- , \quad (1.3a)$$

$$HK^{0*} \rightarrow \Sigma^- p K^+ \pi^- . \quad (1.3b)$$

This paper is organized as follows. In Sec. II, we discuss the mechanisms for H production with Σ^- or Ξ^- beams, focusing on baryon exchange. In Sec. III, we present a capsule résumé of the data on the $p+p \rightarrow \pi^+ + d, \rho^+ + d$ reactions, which provides the cross-section scale for our discussion of the H . Our estimates for the ratio of the H and d cross sections are presented in Sec. IV. The experimental feasibility of H experiments with hyperon beams is assessed in Sec. V, and some conclusions and outlook are provided in Sec. VI.

II. MECHANISMS FOR H PRODUCTION WITH HYPERON BEAMS

The simplest mechanism for H production with Σ^- or Ξ^- beams is baryon exchange, depicted in Fig. 1. We show only the lowest-mass SU(3)-octet exchange, as only an octet can combine with the target octet baryon to form the singlet H . Even as one proceeds to higher energies, the amplitude is therefore built up from only the lowest-mass exchange octet trajectories, rather than the full Regge trajectories. Since the deuteron is an isospin singlet, only $T = \frac{1}{2}$ exchanges are allowed. In addition, triangle diagrams can contribute; these involve meson-baryon scattering as well as baryon-baryon fusion to form the composite object (d or H). For laboratory momenta up to 10 GeV/c or so, these mechanisms have been evaluated for the $p+p \rightarrow \pi^+ + d$ reaction by several authors [27–29]. These simple nucleon/pion exchange models enjoy some success below about 3 GeV/c, but start to break down at higher momenta. A Reggeized baryon-

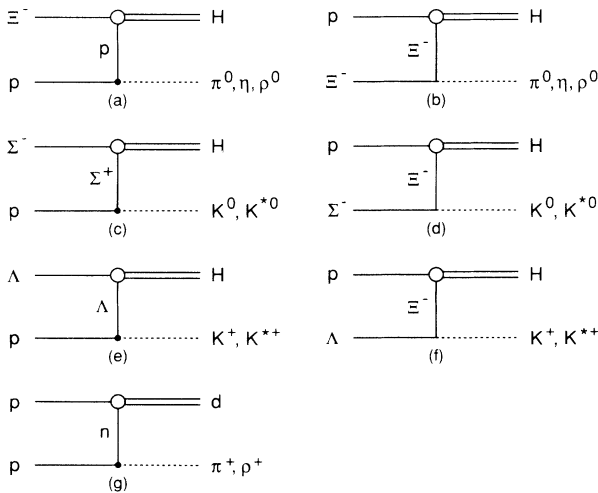


FIG. 1. Baryon-exchange mechanisms for H dibaryon production in hyperon-nucleon interactions (a–f) and deuteron formation in proton-proton collisions (g).

exchange model has been developed by Barger and Michael [30] and applied to the existing $p+p \rightarrow \pi^+ + d$ data up to 21 GeV/c. This model, which includes exchange-degenerate $N_\alpha(\frac{1}{2}^+, \frac{5}{2}^+, \frac{9}{2}^+, \dots)$ and $N_\gamma(\frac{3}{2}^+, \frac{7}{2}^+, \dots)$ trajectories, is rather successful in fitting the data. Thus, for our estimates of ratios of H to d two-body production cross sections, we assume that Reggeized baryon exchange is the dominant process. We use the exchanges shown in Fig. 1 to obtain ratios, since the wave functions for virtual (but almost on-shell) decay of the d or H involve only couplings to SU(3)-octet baryons. At high energies, the exchanged baryon is far off shell, and there will be a large form factor suppressing the baryon-baryon fusion into the composite d or H . We assume that this form-factor effect cancels out in the H/d total cross-section ratio, and that the spin-flavor factors which characterize the lowest-mass exchanges remain the same for the higher-spin Regge exchanges.

At higher energies, the two-body cross sections drop off rapidly, and d or H production will be accompanied by a number of pions $n_\pi \gg 1$. Thus, one would search for the H in the inclusive processes $\Sigma^- p, \Xi^- p \rightarrow HX$ or the semi-inclusive reactions depicted in Fig. 2. A promising reaction in the high-energy regime is

$$\Xi^- + p \rightarrow H + \bar{p} + X . \quad (2.1)$$

The production of an antiproton along with the H is due to the local conservation of baryon number [31]. The exchanged object in Figs. 2(a)–2(c) is the Pomeron [32], which provides the nearly energy-independent (slightly rising) part of the cross section at large \sqrt{s} ; other mechanisms lead to cross sections which drop off as s^{-n} ($n=3$ for Fig. 1, for instance). In Fig. 2, the Pomeron dissolves into a baryon-antibaryon pair with vacuum quantum numbers ($J^{\pi C}=0^{++}, I=0$). The QCD structure of the Pomeron and its strong coupling to quarks is a subject of recent interest [32]. Thus, in Fig. 2(b), we do not obtain a $\Sigma^+ \bar{\Lambda}$ contribution, which would provide a better experimental signature. In Fig. 2(a), for a 600 GeV Ξ^- , the

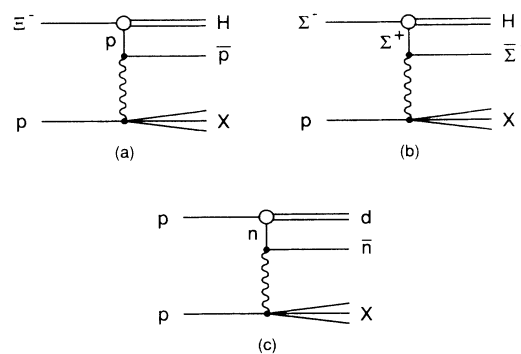


FIG. 2. Pomeron-exchange (wavy line) mechanism for H dibaryon (a),(b) and deuteron (c) production in baryon-baryon collisions. The coupling of the Pomeron to baryon-antibaryon pairs implies that the H or d is produced in association with an antibaryon.

final H should take roughly 400 GeV of the energy, leaving 100 GeV for the \bar{p} and 100 GeV for the X . The \bar{p} will be produced at low x ($\frac{1}{6}$ to $\frac{1}{2}$), along with an H at high x in a sizable number of events. This could provide an important experimental tag of H production. The \bar{p} and reconstructed H momenta should project back to the same point in the target nucleus. One would then look for the final state $\Sigma^- + p + \bar{p}$ after the decay $H \rightarrow \Sigma^- + p$. We return to the experimental aspects in Sec. V.

III. RÉSUMÉ OF THE $p + p \rightarrow \pi^+ + d, \rho^+ + d$ DATA

Our strategy is to estimate an H/d ratio, so we summarize here the salient features of the existing data on deuteron production. The two-body reactions $p + p \rightarrow \pi^+ + d, \rho^+ + d$ have been studied up to laboratory momenta p_L of 24 GeV/c. Data near 5 GeV/c are of interest since this is the momentum region where we could obtain tagged hyperon fluxes with meson beams. Data above 10 GeV/c are due to Anderson *et al.* [33], Baker *et al.* [34], Allaby *et al.* [35], and Amaldi *et al.* [36]. The data at 21.1 GeV/c ($\sqrt{s} = 6.43$ GeV/c²) and 24 GeV/c ($\sqrt{s} = 6.84$ GeV/c²) are of particular interest, since this corresponds to the region of momentum where one might construct a usable Σ^- beam at the Brookhaven AGS or at the proposed KAON facility at TRIUMF.

Above a few GeV/c, the c.m. differential cross sections $d\sigma/d\Omega$ for $p + p \rightarrow \pi^+ + d, \rho^+ + d$ exhibit an approximately exponential dependence on the deuteron transverse momentum $p_T = p \sin\theta_L$, where p is the deuteron laboratory momentum, i.e.,

$$\frac{d\sigma}{d\Omega} = A \exp(-bp_T). \quad (3.1)$$

For the data above 10 GeV/c, the fitted values [36] of A and b as functions of p_L are collected in Table I for the $d + \pi^+$ final state. The geometrical parameter b is essentially independent of \sqrt{s} in this energy region and of order $b \simeq 1$ fm⁻¹. The value of A drops rapidly with \sqrt{s} approximately as

$$A(s) = A(s_0) \left(\frac{s_0}{s} \right)^3. \quad (3.2)$$

At 5 GeV/c, the $\rho^+ + d$ cross section at $p_T \simeq 0$ is about $\frac{1}{5}$ of that for $\pi^+ + d$. At 21 GeV/c, the two cross sections are comparable [35], i.e., $A = 0.32 \pm 0.08$ $\mu\text{b/sr}$, $b = 183 \pm 10$ MeV/c for $\rho^+ + d$, almost the same as the values given in Table I for $\pi^+ + d$. The total cross sec-

TABLE I. Parameters of exponential fit of Eq. (3.1) to differential cross sections for $p + p \rightarrow d + \pi^+$ (from Amaldi *et al.* [36]).

p_L (GeV/c)	A ($\mu\text{b/sr}$)	b (MeV/c)
10	1.5 ± 0.3	183 ± 9
14.2	0.74 ± 0.17	166 ± 11
19.2	0.24 ± 0.06	185 fixed
21.1	0.28 ± 0.05	192 ± 8
24.0	0.16 ± 0.03	185 ± 4

tions at 21 GeV/c are [35]

$$\begin{aligned} \sigma_{\text{tot}}(p + p \rightarrow \pi^+ + d) &= 15.2 \pm 1.5 \text{ nb}, \\ \sigma_{\text{tot}}(p + p \rightarrow \rho^+ + d) &= 15.2 \pm 2.4 \text{ nb}. \end{aligned} \quad (3.3)$$

A comparison of these two reactions at fixed four-momentum transfer $t=0$ yields [36]

$$\left. \frac{d\sigma}{dt} \right|_{t=0} \sim s^{-n}, \quad (3.4)$$

with $n = 3.5 \pm 0.1$ for $\pi^+ + d$ and $n = 2.5 \pm 0.1$ for $\rho^+ + d$. Thus, the $t=0$ cross section for $\rho^+ + d$ decreases less rapidly than that for $\pi^+ + d$, and becomes significantly larger than the π^+ cross section above 20 GeV/c.

The strong s dependence of the $p + p \rightarrow \pi^+ + d, \rho^+ + d$ cross sections is a signature of a baryon-exchange mechanism [37]. The s^{-3} dependence is consistent with Reggeized baryon exchange. The simplest description in terms of Reggeized nucleon exchange fails, since it predicts a strong dip in the angular distribution which is not observed (analogous to the strong dip observed in $\pi^+ + p$ scattering). This led Barger and Michael [30] to an exchange-degenerate Regge model with (N_α, N_γ) trajectories, which reproduces the energy dependence and smooth angular distributions observed for the $p + p \rightarrow \pi^+ + d$ reaction.

The two-body final states $\pi^+ + d, \rho^+ + d$ represent only a small fraction of the inclusive $p + p \rightarrow d + X$ cross section, which displays a broad peak [35] at a deuteron momentum of 10 GeV/c and a peak cross section of 100 $\mu\text{b/sr}$ GeV at $p_L = 21$ GeV/c, $\theta_L = 40$ mrad. From this, we estimate an integrated inclusive cross section of order 1 mb/sr, corresponding to a ratio at small angles of

$$\frac{d\sigma}{d\Omega}(p + p \rightarrow \pi^+ + d) / \frac{d\sigma}{d\Omega}(p + p \rightarrow d + X) \simeq 3 \times 10^{-4}. \quad (3.5)$$

Assuming that the same ratio roughly holds for total cross sections, we estimate (at 21 GeV/c)

$$\sigma_{\text{tot}}(p + p \rightarrow d + X) \simeq 50 \mu\text{b}, \quad (3.6)$$

and hence

$$\frac{\sigma_{\text{tot}}(p + p \rightarrow d + X)}{\sigma_{\text{tot}}(p + p \rightarrow X)} \simeq 10^{-3}. \quad (3.7)$$

This ratio does not seem unreasonable since it is also of the order of a typical coalescence probability, as calculated for instance in thermal models of composite particle formation [24,25,38].

If we now use an s^{-3} dependence [Eq. (3.2)] to extrapolate the values of Eq. (3.3) to 350 GeV/c, a momentum at which Σ^- and Ξ^- beams are available [39] at CERN, we obtain a suppression factor of about $(\frac{1}{4})^6$, or

$$\sigma_{\text{tot}}(p + p \rightarrow \pi^+ + d) \simeq 4 \text{ pb}. \quad (3.8)$$

Since the H cross sections are further suppressed by at least an order of magnitude with respect to d formation, as we demonstrate in the next section, it does not appear

feasible to measure H production via two-body reactions (H + meson) at CERN [39] or Fermilab [40] energies. However, the cross section for inclusive $p + p \rightarrow d + X$ should not drop off rapidly with \sqrt{s} . Hence we expect that $\Sigma^- + p, \Xi^- + p \rightarrow H + X$ would also have measurable rates.

IV. ESTIMATES OF CROSS-SECTION RATIOS

It is very difficult to calculate the absolute value of the cross section for a process like $\Sigma^- + p \rightarrow H + K^{0*}$ from first principles. Hence we use the experimental data on the production of the only known dibaryon, namely, the deuteron, to estimate the H/d ratio. The available data on the reactions $p + p \rightarrow d + \pi^+, d + \rho^+$ were reviewed in the previous section. Here we estimate cross-section ratios for hyperon reactions near 5 and 20 GeV.

We first consider the spin-flavor factors. The deuteron is an object with even parity, spin 1 and isospin 0, corresponding to a 1S_1 - 3D_1 bound state of the np system. Thus, if we consider the fusion of an np pair in an even-parity partial wave with a statistical distribution of spin to form the deuteron, as in Fig. 1(g), the appropriate spin-flavor weight factor $\alpha(n + p \rightarrow d)$ for the $np \rightarrow d$ vertex is given by

$$\alpha(n + p \rightarrow d) = \frac{3}{4} \times \frac{1}{2}. \quad (4.1)$$

The short-range part of the wave function of the H dibaryon, if it is strongly bound, corresponds to an even-parity SU(3) singlet, with spin 0. Since a singlet couples to each allowed baryon-baryon charge state with equal weight, and there are eight combinations $\Lambda\Lambda, \Sigma^0\Sigma^0, \Sigma^+\Sigma^-, \Sigma^-\Sigma^+, \Xi^-p, p\Xi^-, \Xi^0n, n\Xi^0$, each channel has a flavor factor $\frac{1}{8}$ corresponding to

$$\alpha(B_1 + B_2 \rightarrow H) = \frac{1}{4} \times \frac{1}{8} = \frac{1}{32}. \quad (4.2)$$

The spin factor is always $\frac{1}{4}$ (the probability of spin 0 in a statistical distribution of baryon-baryon spins). Note that in the graphs of Fig. 1, only one ordering for baryon-baryon fusion occurs, so the flavor factor is not doubled to $\frac{1}{4}$ for nonidentical baryons. For example, in Fig. 1(c), the $\Sigma^-\Sigma^+$ ordering occurs, but not $\Sigma^+\Sigma^-$. This is in contrast to the situation in a heavy-ion collision, where one could produce a Σ^+ and a Σ^- in separate nucleon-nucleon collisions, followed by the fusion process $\Sigma^+\Sigma^- \rightarrow H$ or $\Sigma^-\Sigma^+ \rightarrow H$; here both orderings occur. The same argument results in the flavor factor of $\frac{1}{2}$ in Eq. (4.1), since in Fig. 1(g) only the ordering $pn \rightarrow d$ occurs. We do not attempt to refine our rough estimate here, but note that a more detailed group-theoretical calculation based on the color-spin-flavor group SU(18), including quark antisymmetrization, may modify our results somewhat, since the fusion weights will not factorize in general into a spin and flavor factor [41].

We note that there are angular momentum and parity selection rules for the reaction

$$Y + p \rightarrow H + \text{PS}, \quad (4.3)$$

where Y is a positive-parity spin- $\frac{1}{2}$ hyperon and PS is a pseudoscalar meson. Restrictions arise because both

final-state particles have spin 0. The final state must have unnatural parity, and this requires the initial hyperon-nucleon state to be in the triplet spin state. The allowed initial states ${}^{2S+1}L_J$ are listed in Table II for several values of the final-state orbital angular momentum l . For $p + p \rightarrow d + \pi^+$, both singlet (odd- l) and triplet (even- l) initial spin states occur. Note also that, if we are considering a baryon-exchange reaction with the meson emitted in the forward direction, the projection of the angular momentum on the direction of the incident momentum must be zero. This means that only the initial state with total spin 1 and projection 0 on the momentum can contribute to the reaction where the meson goes directly forward and the H directly backward in the center-of-mass system. Note that these selection rules do not hold for deuteron production or for reactions producing vector mesons because the deuteron and the vector meson both have spin 1, and there are many more allowed angular momentum couplings.

The other ingredients in computing H/d ratios are the coupling constants at the meson emission vertex [see Figs. 1(a)–1(g)]. We first assume that SU(3) symmetry is valid, which yields the relations

$$g_{NN\pi} = -g_{\Xi\Sigma K} = g, \quad (4.4a)$$

$$g_{\Sigma NK} = -g_{\Xi\Xi\pi} = g(1 - 2\alpha_{\text{PS}}), \quad (4.4b)$$

$$g_{\Lambda NK} = g_{\Xi\Xi\eta_8} = -g(1 + 2\alpha_{\text{PS}})/\sqrt{3}, \quad (4.4c)$$

$$g_{\Xi\Lambda K} = g_{NN\eta_8} = g(4\alpha_{\text{PS}} - 1)/\sqrt{3}, \quad (4.4d)$$

$$g_{NN\eta_1} = g_{\Xi\Xi\eta_1} = \sqrt{2}g_{NN\eta_8} \quad (4.4e)$$

for pseudoscalar mesons, where α_{PS} is the F/D ratio. Here the SU(3)-singlet and -octet states are

$$\eta_1 = (u\bar{u} + d\bar{d} + s\bar{s})/\sqrt{3},$$

$$\eta_8 = (u\bar{u} + d\bar{d} - 2s\bar{s})/\sqrt{6},$$

and we have used the Okubo-Zweig-Iizuka rule ($g_{NN\eta_8} = 0, \eta_8 = s\bar{s}$) to relate the η_1 and η_8 couplings as per Eq. (4.4e). For vector mesons, we have both electric (g -type) and magnetic (f -type) couplings, with corresponding F/D ratios α_V^e and α_V^m . For static SU(6) symmetry, for instance, we have

$$\alpha_V^e = 1, \quad \alpha_V^m = \frac{2}{5}, \quad \alpha_{\text{PS}} = \frac{2}{5}. \quad (4.5)$$

In one-boson-exchange models, which are fitted to the observed $NN, \Lambda N,$ and ΣN scattering data, one preserves SU(3) symmetry and entertains deviations from SU(6).

TABLE II. Allowed initial states for production of the deuteron and H dibaryon for several values of final-state relative orbital angular momentum l .

l	$p + p \rightarrow d + \pi^+$	$Y + p \rightarrow H + \text{PS}$
0	3P_1	3P_0
1	${}^1S_0, {}^1D_2$	3S_1
2	${}^3P_1, {}^3PF_2, {}^3F_3$	3PF_2

For instance, in model D of the Nijmegen group [42], one obtains

$$\alpha_V^e = 1, \quad \alpha_V^m = 0.334, \quad \alpha_{PS} = 0.485, \quad (4.6)$$

which is not too far from the SU(6) limit. However, the data on ΛN and ΣN scattering are limited, so this is not a good test of SU(6). From studies of Σ and Λ production [43], it is known that the strong Σ suppression predicted in SU(6) is not seen experimentally, i.e., the ratio $g_{\Sigma NK}^2/g_{\Lambda NK}^2$ extracted from the data is much larger than the SU(6) prediction of $\frac{1}{27}$, which follows from Eqs. (4.4b) and (4.4c) with $\alpha_{PS} = \frac{2}{5}$. Information is also available on Σ and Λ couplings from analyses of $\bar{K}N$ dispersion relations; Baillon *et al.* [44] obtain $g_{\Sigma NK}^2 = 0.8 \pm 3.2$, $g_{\Lambda NK}^2 = 21.3 \pm 3.7$. This suggests that a ratio as large as $g_{\Sigma NK}^2/g_{\Lambda NK}^2 = \frac{1}{2}$ is allowed, corresponding to $\alpha_{PS} \approx 0.28$. In our later estimates of cross-section ratios, we thus adopt a range of values $\frac{1}{4} \leq \alpha_{PS} \leq \frac{2}{5}$.

In the limit of SU(3) symmetry, certain relations between cross sections follow from the fact that a deeply bound H is an SU(3) singlet. For instance, neglecting mass differences within the baryon and meson octets, and retaining only the dependence of the amplitude T on coupling constants, we obtain

$$\begin{aligned} T(\Xi^- + p \rightarrow H + \pi^0) &= g_{\Xi^- p H} g_{pp\pi^0} + g_{\Xi^- p H} g_{\Xi^- \Xi^- \pi^0} \\ &= 2\alpha_{PS} g_{\Xi^- p H} g, \end{aligned} \quad (4.7a)$$

$$\begin{aligned} T(\Sigma^- + p \rightarrow H + K^0) &= g_{\Sigma^- \Sigma^+ H} g_{\Sigma^+ p K^0} + g_{\Xi^- p H} g_{\Xi^- \Sigma^- K^0} \\ &= \sqrt{2}g [g_{\Sigma^- \Sigma^+ H} (1 - 2\alpha_{PS}) - g_{\Xi^- p H}], \end{aligned} \quad (4.7b)$$

$$\begin{aligned} T(\Lambda + p \rightarrow H + K^+) &= g_{\Lambda \Lambda H} g_{\Lambda p K^+} + g_{\Xi^- p H} g_{\Xi^- \Lambda K^+} \\ &= \frac{g}{\sqrt{3}} [-g_{\Lambda \Lambda H} (1 + 2\alpha_{PS}) + g_{\Xi^- p H} (4\alpha_{PS} - 1)] \end{aligned} \quad (4.7c)$$

by adding coherently the two graphs of Fig. 1 which contribute to each channel, and using Eq. (4.4). For the H , each baryon-baryon charge state configuration has the same coupling strength, up to a phase. In a consistent

phase convention, we have $g_{\Xi^- p H} = g_{\Sigma^- \Sigma^+ H} = -g_{\Lambda \Lambda H} = g_H$, so the amplitudes (4.7) are all proportional to $\alpha_{PS} g_H$, and we find the cross-section relations

$$\sigma(\Sigma^- + p \rightarrow H + K^0) = \frac{2}{3} \sigma(\Lambda + p \rightarrow H + K^+), \quad (4.8a)$$

$$\sigma(\Sigma^- + p \rightarrow H + K^0) = 2\sigma(\Xi^- + p \rightarrow H + \pi^0) \quad (4.8b)$$

in the SU(3) limit. Note that Eqs. (4.8a) and (4.8b) are independent of α_{PS} , so we do not need to assume the validity of SU(6). Similar relations hold for vector-meson production. Of course, SU(3) symmetry is broken, and the $\Sigma^- + p$ and $\Lambda + p$ reactions are suppressed with respect to $\Xi^- + p$ by a factor $\lambda = P(s\bar{s})/P(u\bar{u})$, which represents a penalty factor for producing an additional strange-quark ($s\bar{s}$) pair in the final state. From a number of measurements of the ratio of probabilities P for $s\bar{s}$ vs $u\bar{u}$ production [45], we estimate $\lambda \approx \frac{1}{5}$ at the \sqrt{s} values under consideration. We do not consider other mechanisms for SU(3) breaking. For instance, one possibility is an $L=2$ decuplet admixture analogous to the D -wave mixing in the deuteron. This would affect the Σ and Ξ couplings, but not the N and Λ , where such mixing is forbidden by isospin conservation.

We now estimate the H/d ratio. Including only the dependence on coupling constants as in Eq. (4.7), we have

$$T(p + p \rightarrow d + \pi^+) = \sqrt{2}g_{pn\pi} + g_{npd} = 2g_{npd}g. \quad (4.9)$$

The extra $\sqrt{2}$ in Eq. (4.9) arises from the Pauli principle. In addition to the dependence on coupling constants exhibited above, the cross-section ratio also includes a spin factor which favors the production of the spin-1 deuteron. Thus,

$$\begin{aligned} \frac{\sigma(\Xi^- + p \rightarrow H + \pi^0)}{\sigma(p + p \rightarrow d + \pi^+)} &= \frac{\sigma(\Xi^- + p \rightarrow H + \rho^0)}{\sigma(p + p \rightarrow d + \rho^+)} \\ &= \alpha_{PS}^2 \frac{\alpha(\Xi^- + p \rightarrow H)}{\alpha(n + p \rightarrow d)} \\ &= \alpha_{PS}^2 / 12 \approx (5-13) \times 10^{-3}. \end{aligned} \quad (4.10)$$

We can also estimate the production of the η relative to π^0 . Using $|\eta\rangle = \cos\theta_{PS}|\eta_8\rangle - \sin\theta_{PS}|\eta_1\rangle$, we obtain

$$\begin{aligned} \frac{\sigma(\Xi^- + p \rightarrow H + \eta)}{\sigma(\Xi^- + p \rightarrow H + \pi^0)} &= \left[\frac{g_{pp\eta} + g_{\Xi^- \Xi^- \eta}}{g_{pp\pi^0} + g_{\Xi^- \Xi^- \pi^0}} \right]^2 = \frac{1}{3} \left[\frac{(\alpha_{PS} - 1)\cos\theta_{PS} + \sqrt{2}(1 - 4\alpha_{PS})\sin\theta_{PS}}{\alpha_{PS}} \right]^2 \\ &= \begin{cases} 2.65 & (\alpha_{PS} = \frac{1}{4}), \\ 0.16 & (\alpha_{PS} = \frac{2}{5}), \end{cases} \end{aligned} \quad (4.11)$$

where we have assumed a pseudoscalar mixing angle of $\theta_{PS} = -20^\circ$. Thus η production is comparable to π^0 production. In both cases, one would search for the two photon decays ($\pi^0 \rightarrow 2\gamma, \eta \rightarrow 2\gamma$), but this would be more difficult than detecting a final state composed only of charged particles. We also note that

$$\sigma(\Xi^- + n \rightarrow H + \pi^-) = 2\sigma(\Xi^- + p \rightarrow H + \pi^0), \quad (4.12)$$

since the final state has isospin 1. The $\Xi^- + n \rightarrow H + \pi^-$ process would enter in the two-step process $K^- + d \rightarrow K^+ + \pi^- + H$ after an initial $K^- + p \rightarrow K^+ + \Xi^-$ reaction.

In the 20 GeV/c region, the $p+p \rightarrow \pi^+ + d, \rho^+ + d$ cross sections are about equal. Using Eqs. (4.8a) and (4.8b), with a factor $\lambda \simeq \frac{1}{5}$ included on the right-hand side of (4.8b), together with Eqs. (3.3) and (4.10), with $\alpha_{PS} = \frac{2}{5}$, we obtain the rough estimates

$$\sigma(\Xi^- + p \rightarrow H + \pi^0) \simeq \sigma(\Xi^- + p \rightarrow H + \rho^0) \simeq 0.2 \text{ nb} , \quad (4.13a)$$

$$\sigma(\Sigma^- + p \rightarrow H + K^0) \simeq \sigma(\Sigma^- + p \rightarrow H + K^{0*}) \simeq 0.08 \text{ nb} , \quad (4.13b)$$

$$\sigma(\Lambda + p \rightarrow H + K^+) \simeq \sigma(\Lambda + p \rightarrow H + K^{*+}) \simeq 0.12 \text{ nb} . \quad (4.13c)$$

We have so far neglected effects due to the differing sizes (rms radius) of the d and H . If the H is deeply bound, it will be a smaller object than the d , with a size approaching that of a proton. This difference would be reflected in a different slope parameter b in Eq. (3.1). The volume in momentum space for H formation depends on k_H^3 , while for d formation it is k_d^3 , where k_d and k_H are the relative momenta (inverse ranges) characteristic of the deuteron or H wave functions. For the d we expect $k_d \simeq 150 \text{ MeV}/c$, while for the H a higher value (perhaps $k_H \simeq 0.3 \text{ GeV}/c$ corresponding to shorter range) may be required. This size effect could enhance the H/d ratio given above by a considerable factor. In what follows, we do not include this possible size enhancement factor, so our results may be regarded as conservative.

In our estimates, we have assumed that the d and H production reactions have the same kinematical form factors. To see that this is not unreasonable, consider the $p+p \rightarrow d + \rho^+$ and $\Xi^- + p \rightarrow H + \rho^0$ reactions at $p_L = 20 \text{ GeV}/c$, corresponding to initial- and final-state c.m. momenta $(k, q) = (3.0, 2.8)$ and $(2.95, 2.74) \text{ GeV}/c$, respectively. The c.m. momentum transfer $k - q$ for 0° production is then practically the same (200 MeV/c) for the two reactions.

In the above, we assumed that the H is an SU(3) unitary singlet [see Eq. (4.2)]. If the H is weakly bound, i.e., deuteronlike, its wave function will be dominated by the nearest threshold, namely the $\Lambda\Lambda$ channel. In this case, the $\Lambda + p \rightarrow H + K^+, H + K^{*+}$ reactions dominate, since only these involve $\Lambda\Lambda$ fusion. If the H is a weakly bound $\Lambda\Lambda$ state, we expect

$$\frac{\sigma(\Lambda + p \rightarrow H + K^+)}{\sigma(p + p \rightarrow d + \pi^+)} \simeq \left[\frac{1 + 2\alpha_{PS}}{12} \right]^2 \simeq \frac{9}{4} \times 10^{-2} \quad (4.14)$$

for $\alpha_{PS} \simeq \frac{2}{5}$.

Let us now consider H production with hyperon beams at lower momentum in the few GeV/c region. The $p+p \rightarrow d + \pi^+$ reaction displays a peak cross section [46] of 3.1 mb at a laboratory energy of 585 MeV ($p_L = 1.2 \text{ GeV}/c$). This quasisymmetric peak has a half-width $\Gamma/2 = (-130, +180) \text{ MeV}$; at the peak, the $p+p \rightarrow d + \pi^+$ reaction contributes 28% of the total inelastic cross section [46]. The peak cross section occurs at a total c.m. energy \sqrt{s} given by

$$\sqrt{s} - \sqrt{s_0} \simeq m_\pi , \quad (4.15)$$

where $\sqrt{s_0} = m_d + m_{\pi^+}$ is the threshold energy. That is, the $p+p \rightarrow d + \pi^+$ cross section peaks at an energy corresponding to the threshold for producing one additional pion ($pp \rightarrow NN\pi\pi$). If we assume that Eq. (4.15) also holds for the other two-body channels under consideration, we arrive at Table III, which gives the thresholds and predicted peak momenta. The $\Lambda p \rightarrow HK^+, HK^{*+}$ values are very similar to those for the $\Sigma^- p$ reactions. We have used the centroid masses $m_\rho \simeq 0.77 \text{ GeV}$, $m_{K^*} \simeq 0.89 \text{ GeV}$ for these calculations; of course, the finite widths of these mesons will spread out the thresholds and peaks. In Table III, we have used a mass $m_H = 2.15 \text{ MeV}$; as m_H varies from 2.05 to 2.23 GeV, the peak momentum for $\Xi^- + p \rightarrow H + \pi^0$ varies from 0.64 to 1.4 GeV/c and that for $\Sigma^- + p \rightarrow H + K^0$ from 2.5 to 3.0 GeV/c.

Using Eqs. (4.8) and (4.10), we then estimate the peak total cross sections for an SU(3) singlet H :

$$\begin{aligned} \sigma(\Xi^- + p \rightarrow H + \pi^0) &\simeq \frac{1}{75} \times 3 \text{ mb} \simeq 40 \mu\text{b} \quad (\text{at } 1.1 \text{ GeV}/c) , \\ \sigma(\Sigma^- + p \rightarrow H + K^0) &\simeq 2\lambda \times 40 \mu\text{b} \simeq 16 \mu\text{b} \\ &\quad (\text{at } 2.8 \text{ GeV}/c) , \\ \sigma(\Lambda + p \rightarrow H + K^+) &\simeq 24 \mu\text{b} \quad (\text{at } 2.8 \text{ GeV}/c) . \end{aligned} \quad (4.16)$$

The estimate of vector-meson production cross sections in the few GeV/c region is more delicate. The $p+p \rightarrow d + \pi^+ + \pi^0$ cross section [46] displays a peak value of 0.4 mb at a laboratory kinetic energy of 1.5 GeV ($p_L \simeq 2.3 \text{ GeV}/c$). Unfortunately, this peak cannot be interpreted in terms of the $p+p \rightarrow d + \rho^+$ reaction, since it occurs for a value of p_L below the nominal threshold at 2.6 GeV/c for ρ production (Table III). Most likely, this peak arises from a Δ production mechanism, for instance, $p+p \rightarrow \Delta^+ + \Delta^+ \rightarrow (\pi^+ n) + (\pi^0 p) \rightarrow \pi^+ \pi^0 d$; the $\Delta\Delta$ threshold is near 2.1 GeV/c. Thus, the ratio of $d + \pi^+$ and $d + \rho^+$ total cross sections cannot be easily extracted from the data at low momenta. However, according to the data of Amaldi *et al.* [36] and Anderson *et al.* [33], the ratio of $d + \rho^+$ and $d + \pi^+$ differential cross sections at $p_T = 0$ [see Eq. (3.1)] is about $\frac{1}{5}$ at $p_L = 5 \text{ GeV}/c$. At lower momenta, this ratio would become even smaller. A reasonable guess in the few GeV/c regime is

TABLE III. Threshold and predicted peak values of laboratory momenta p_L for d or H production reactions for $m_H = 2.15 \text{ GeV}$.

Reaction	Threshold (GeV/c)	Peak (GeV/c)
$pp \rightarrow d\pi^+$	0.8	1.2
$pp \rightarrow d\rho^+$	2.6	3.1
$\Xi^- p \rightarrow H\pi^0$	0.4	1.1
$\Xi^- p \rightarrow H\rho^0$	2.9	3.3
$\Sigma^- p \rightarrow HK^0$	2.2	2.8
$\Sigma^- p \rightarrow HK^{0*}$	3.6	4.1

$$\frac{\sigma(Y+p \rightarrow H+V)}{\sigma(Y+p \rightarrow H+PS)} \sim \frac{1}{10}, \quad (4.17)$$

where the cross sections are taken at the same available c.m. energy $\sqrt{s} - \sqrt{s_0}$ (for example, $\Sigma^- + p \rightarrow H + K^{0*}$ at 4.1 GeV/c is compared to $\Sigma^- + p \rightarrow H + K^0$ at 2.8 GeV/c).

In the few GeV/c region, it is not feasible to produce sufficiently intense hyperon beams to measure processes like $Y+p \rightarrow H+M$ directly as single-step reactions. Rather, a tagged hyperon is produced by a meson (π or K) impinging on a hydrogen or nuclear target, and then interacts with a second proton in the same hydrogen target or even in the same nucleus.

Finally, we obtain a crude estimate of the cross section for reaction (2.1), starting with the ratio

$$\frac{\sigma(\Xi^- + p \rightarrow H + \bar{p} + X)}{\sigma(p + p \rightarrow d + \bar{n} + X)} \simeq \frac{1}{3} \frac{g_{\Xi^- p H}^2}{g_{npd}^2} = \frac{1}{12}. \quad (4.18)$$

As discussed earlier, the size effect could significantly enhance this ratio. There are no measurements of deuteron production in coincidence with an antinucleon. To get an order of magnitude estimate, we assume that Eq. (3.7) holds at high energy, and that the $(d + \bar{n} + X)/(d + X)$ ratio is in the range 0.1–0.5. Then we obtain

$$\sigma(\Xi^- + p \rightarrow H + \bar{p} + X) \simeq 0.4\text{--}2 \mu\text{b}. \quad (4.19)$$

The corresponding cross section for $\Sigma^- + p \rightarrow H + \bar{\Sigma}^- + X$ ($\bar{\Sigma}^-$ is the antiparticle of Σ^+) should be about the same as (4.19). If the $\bar{\Sigma}^-$ does not decay and is detected magnetically, it will be indistinguishable from the large flux of Σ^- 's associated with the beam. If it does decay, reconstruction of the decay $\bar{\Sigma}^- \rightarrow \pi^- \bar{n}$ is much more difficult than detecting a \bar{p} .

V. EXPERIMENTAL CONSIDERATIONS

We now evaluate the prospects for producing an H with real hyperon beams at 20 GeV/c and above, and tagged hyperons at lower momentum produced with meson beams. In the latter case, we consider sequential reactions with pion and kaon beams incident on a liquid hydrogen or deuterium target. The reaction on the first proton produces a tagged hyperon, which then interacts with a second proton in the same hydrogen target to produce an H . We first examine reactions on the two protons leading to an H plus three charged mesons. The sequential reactions induced by K^- beams are

$$K^- + p \rightarrow \Sigma^- + \pi^+ \quad \text{and} \quad \Sigma^- + p \rightarrow H + K^0, \quad (5.1a)$$

$$K^- + p \rightarrow \Xi^- + K^+ \quad \text{and} \quad \Xi^- + p \rightarrow H + \rho^0, \quad (5.1b)$$

$$K^- + p \rightarrow \Sigma^- + \pi^+ \quad \text{and} \quad \Sigma^- + p \rightarrow H + K^{0*}, \quad (5.1c)$$

$$K^- + p \rightarrow \Lambda + \rho^0 \quad \text{and} \quad \Lambda + p \rightarrow H + K^+, \quad (5.1d)$$

while those initiated by π^- beams are

$$\pi^- + p \rightarrow \Sigma^- + K^+ \quad \text{and} \quad \Sigma^- + p \rightarrow H + K^0, \quad (5.2a)$$

$$\pi^- + p \rightarrow \Lambda + K^0 \quad \text{and} \quad \Lambda + p \rightarrow H + K^+, \quad (5.2b)$$

$$\pi^- + p \rightarrow \Sigma^- + K^+ \quad \text{and} \quad \Sigma^- + p \rightarrow H + K^{0*}, \quad (5.2c)$$

$$\pi^- + p \rightarrow \Lambda + K^{0*} \quad \text{and} \quad \Lambda + p \rightarrow H + K^+. \quad (5.2d)$$

Note that π^+ beams are not useful in experiments with a hydrogen target: although the reaction $\pi^+ + p \rightarrow \Sigma^+ + K^+$ is allowed, the second step $\Sigma^+ + p \rightarrow H + K^+ + \pi^+$ necessarily involves a three-body final state because of charge conservation. If one assumes that the H decay products are not detected, the above reactions are identified by observing three charged mesons in the final state. We observe the weak decay $K^0 \rightarrow K_s \rightarrow \pi^+ \pi^-$, and the strong decays $K^{0*} \rightarrow K^+ \pi^-$ and $\rho^0 \rightarrow \pi^+ \pi^-$. The reactions involving the ρ^0 or K^{0*} could also proceed at higher energies through the $f_2(1270)$ or $K_2^*(1430)$, which are strongly coupled to the same $\pi^+ \pi^-$ and $K^+ \pi^-$ decay channels, respectively. The higher incident energies would allow the use of thicker hydrogen targets, since the associated tagged hyperons would have longer decay lengths. The reaction sequences of Eqs. (5.1) and (5.2) correspond to the overall reactions

$$K^- pp \rightarrow \pi^+ \pi^+ \pi^- H, \quad (5.3a)$$

$$K^- pp \rightarrow \pi^+ K^+ \pi^- H, \quad (5.3b)$$

$$\pi^- pp \rightarrow K^+ \pi^+ \pi^- H, \quad (5.3c)$$

$$\pi^- pp \rightarrow K^+ K^+ \pi^- H. \quad (5.3d)$$

The reactions (5.3a) and (5.3c) involve the weak decay $K_s \rightarrow \pi^+ \pi^-$, so strangeness is not conserved. Note that in reactions (5.1a) and (5.2a), which involve K^0 production, there would be large backgrounds if we do not detect the H , since the $\pi^+ \pi^-$ pair can result from \bar{K}^0 as well as K^0 decay. For instance, the competing process

$$\Sigma^- + p \rightarrow Y^{0*} + n \rightarrow \bar{K}^0 + nn$$

for the second stage of Eqs. (5.1a) and (5.2a) leads to the same $\pi^+ \pi^- \pi^-$ (5.3a) or $K^+ \pi^+ \pi^-$ (5.3c) detected final state. This background would swamp the H signal, unless we also detect the decay $H \rightarrow \Sigma^- p$ to distinguish the H from two-neutron formation. Thus, reactions involving K^+ or K^{0*} formation are preferable to those involving the K^0 .

Experiments with mesons incident on a deuterium target are also worthy of consideration. As in Eqs. (5.1) and (5.2), these are also two-step reactions, where the intermediate-state hyperon is now virtual. The processes which involve only charged mesons in the final state are

$$K^- + d \rightarrow H + K^0, \quad (5.4a)$$

$$K^- + d \rightarrow H + K^{0*}, \quad (5.4b)$$

$$K^- + d \rightarrow H + K^+ + \pi^- (K^+ \pi^- \neq K^{0*}), \quad (5.4c)$$

$$\pi^- + d \rightarrow H + K^{0*} + K^{0*}, \quad (5.4d)$$

$$\pi^+ + d \rightarrow H + K^+ + K^+. \quad (5.4e)$$

Each of these reactions has two contributing amplitudes in which the incident meson interacts with the proton or the neutron. Equations (5.4a) and (5.4b) involve Ξ pro-

duction followed by $\Xi N \rightarrow H$ fusion, while Eqs. (5.4c)–(5.4e) correspond to hyperon production and then $YN \rightarrow KH, K^*H$.

For reaction (5.4a), the differential cross section vanishes if the K^0 emerges at 0° , since a pseudoscalar meson cannot induce the required $d \rightarrow H$ spin-flip transition. This problem does not occur for (5.4b), since the K^{0*} carries the requisite spin; this reaction was discussed by Fitch [47], and a 0° cross section of 40 nb/sr at 3 GeV/c was estimated by Dover [48].

In addition, we consider reactions on a liquid hydrogen target at 20 and 600 GeV/c, respectively, using hyperon beam lines:

$$\Sigma^- + p \rightarrow K^{0*} + H, \quad (5.5a)$$

$$\Xi^- + p \rightarrow H + \bar{p} + X. \quad (5.5b)$$

For experiments with hyperons, the optimum reaction and incident energy (for signal to background) depends on the beam intensity and purity, the hyperon (Ξ, Σ, Λ) production cross sections, the expected background rates, the H production thresholds and cross sections, and the detector configuration and thresholds. The momentum of 20 GeV/c appears reasonable for a hyperon-beam experiment, and is determined by balancing the decreasing H production cross section in two-body reactions with the increasing hyperon flux (decay length) at higher energy. At an incident hyperon momentum of 600 GeV/c, the final-state Σ^- from the decay $H \rightarrow \Sigma^- p$ lives long enough for detection in a magnetic spectrometer.

In reactions (5.3a)–(5.3d) and (5.5a) above, we assume that the H decay products are not detected. Therefore, the two-body nature of the reaction is very important. For example, in reactions involving a ρ^0 , one measures the decay products π^+ and π^- and determines the ρ^0 -invariant mass. One should obtain a peak in the missing mass spectrum if the H is indeed bound and produced in a two-body reaction. For Eq. (5.5b), we require detection of the H decay products. For the bound H , the feasibility of detecting its decay products depends on the decay length $L_D = \beta\gamma c\tau$ of the H itself and of its decay product Σ^- , on the acceptance of the detector, and on the quality of the particle identification for beam and detected particles. If L_D is too large, the H will pass through the apparatus without decaying, and hence elude detection. For an unbound H or an excited state H^* , one could also observe charged particles from the decays $H \rightarrow \Lambda\Lambda$, $\Xi^- p \rightarrow p\pi^- p\pi^-$. The backgrounds for experiments in which the H decay products are also detected should be very low, since the kinematic requirements are very selective. For $H \rightarrow \Sigma^- p$, $\Sigma^- \rightarrow \pi^- n$, the missing energy and momentum must reconstruct to the neutron mass, the neutron and π^- to a Σ^- , the $\Sigma^- p$ to an H mass, and the $\pi^+\pi^-$ to a ρ^0 . The trajectories of the ρ^0 and H must also extrapolate to the point of the target intercepted by the incident and outgoing kaons.

In designing an experiment, one must consider the relative merits of using pion or kaon incident beams. Pion beams have the advantage of much greater intensity and purity than kaon beams, but the H cross sections are smaller with pions. At the proposed KAON facility [49]

the anticipated beam intensities (particles/sec) are 1.5×10^7 (K^-), 1.9×10^9 (π^-), and 3.6×10^9 (π^+) at 6 GeV/c and 6.6×10^7 (K^-), 1.6×10^{10} (π^-), and 2.4×10^{10} (π^+) at 2.5 GeV/c. Thus, the π^+/K^+ ratio is about 360 at 2.5 GeV/c and 240 at 6 GeV/c. For the less pure kaon beam, but not for the pion beam, an in-beam particle identification Cherenkov detector would be required, and this could limit the usable kaon-beam intensity. If a tagging detector system can be designed which tolerates the full pion rate, the tagged hyperon rate would be several hundred times larger with the pion beam than with kaons.

To estimate the signal-to-background ratio, one must consider all reactions that can yield a three-meson trigger without involving H production. For example, the reactions $K^- p \rightarrow \Xi^- \pi^+ \pi^- K^+$ or $K^- p \rightarrow K^- p K^+ K^- \pi^+ \pi^-$ yield the $K^+ \pi^+ \pi^-$ combination. Such reactions will give a continuum background, and our ability to see an H peak in the missing mass spectrum rests on achieving good mass resolution. We note that the background for reactions involving two K^+ mesons in the final state will be smaller than for the other reactions, but the H cross section is also smaller. More detailed estimates will be necessary, but they are beyond the scope of the present work.

It would also be interesting to look for polarization effects in these reactions. For the $\Xi^- + p \rightarrow H + \rho^0$ reaction, for instance, one could determine the ρ^0 polarization from the measured asymmetries in the $\pi^+\pi^-$ final state. The ρ^0 could be polarized even if the Ξ^- beam is unpolarized. One may also exploit the fact that a vector meson produced in association with an H carries different polarization information than one arising from a background process.

A. Reactions with π^\pm and K^- beams on a hydrogen target

As an example, we now consider in more detail the reaction (5.1b), namely, $K^- + p \rightarrow \Xi^- + K^+$ followed by $\Xi^- + p \rightarrow H + \rho^0$. Similar considerations apply to the use of tagged Σ^- 's and Λ 's to produce the H . For instance, the (5.1c) and (5.1d) reactions would be studied simultaneously in the same experimental setup, as they also correspond to $K^- pp \rightarrow K^+ \pi^- \pi^+ H$. The coincidence condition $K^+ \pi^+ \pi^-$ is used, which makes it crucial to have a high detector acceptance. The Λ, Σ^-, Ξ^- decay lengths L_D for a total energy of 4 GeV are 27, 14, 14 cm, while at 1.5 GeV they are 7.1, 2.5, 2.6 cm, respectively. Consequently, tagged Λ 's are more effective than Σ^- or Ξ^- particles. For 1–10 GeV/c K^- 's incident on a liquid hydrogen target, the interaction length L_i is about 1500 cm ($L_i = A/N\rho\sigma$, where N is Avogadro's number, $\rho = 0.063$ gm/cm³ is the density of liquid hydrogen, $\sigma = 35$ mb for the K^- proton total cross section, and $A = 2$ for liquid H₂). If we match the target thickness to the Λ decay length, we have $27/1500 \approx 0.02$, i.e., a 2% interaction length target. Thus, 0.5–2% targets are appropriate in the momentum range 1–10 GeV/c. With a 5.5 GeV/c K^- beam, and a K^+ detected in the laboratory between 40° and 100° , the tagged Ξ^- is emitted between 18° and 5° with momentum from 4.2 to 5.6 GeV/c,

respectively. The need for high-momentum Ξ^- 's follows from the required threshold for producing $H + \rho^0$, i.e., $p_L > 3$ GeV/c from Table III. For a ρ^0 emitted between 0° and 30° , with respect to the Ξ^- direction, the kinetic energy exceeds 1 GeV, and the decay pions are relatively easily detected.

We now make a rough estimate of the count rate for reaction (5.1b) with a 6 GeV/c K^- beam. The combined probability for both interactions in the same 1% target is the product of the individual probabilities; for each reaction, we take a 0.5% interaction length target. We assume a total cross section of 35 mb for K^-p and Ξ^-p interactions, $5 \mu\text{b}$ for the $K^- + p \rightarrow K^+ + \Xi^-$ reaction [50], and $2 \mu\text{b}$ for the $\Xi^- + p \rightarrow H + \rho^0$ reaction, obtained by taking $\frac{1}{2}$ of the predicted peak values of Eqs. (4.16) and (4.17). We assume a 10% acceptance efficiency to account for the fact that we measure only back-angle K^+ events. The probability for the two interactions is then

$$P = 0.005 \times \frac{0.005}{35} \times 0.005 \times \frac{0.002}{35} \times 0.1 = 2 \times 10^{-14} .$$

At the $1.5 \times 10^7 \text{ sec}^{-1}$ K^- -beam rate at 6 GeV/c planned for KAON, one gets roughly 10^{-3} event/h. A more favorable case is reaction (5.1d). The observed [50] $K^- + p \rightarrow \Lambda + \rho^0$ cross section at 6 GeV/c is about $9 \mu\text{b}$, whereas one-half of the predicted peak cross section for $\Lambda + p \rightarrow H + K^+$ is of order $12 \mu\text{b}$. For a 2% target, we obtain $P = 8.8 \times 10^{-13}$, or about 5.4×10^{-2} event/h. At such low rates, an H experiment with K^- beams appears to be marginal.

As mentioned in Sec. IV, the cross section for production of a deeply bound H could be enhanced with respect to that for the deuteron by a geometrical factor $k_H^3/k_d^3 \simeq (\langle r^2 \rangle_d / \langle r^2 \rangle_H)^{3/2}$. If we take $\langle r^2 \rangle_d^{1/2} = 2$ fm and $\langle r^2 \rangle_H^{1/2} \simeq (\frac{6}{3})^{1/3} \langle r^2 \rangle_p^{1/2} \simeq 1$ fm, then this enhancement factor is about 8. If this more optimistic scenario is adopted, we would obtain, from (5.1d), roughly 500 events with an H in a 1000-h run. In this case, the counting rate appears to be acceptable for an experiment with 6 GeV/c K^- beams at KAON.

We now consider the π^- reactions (5.2a)–(5.2d) at 6 GeV/c. The dominant processes turn out to be (5.2b) and (5.2d), which involve vector-meson production in the first step. The relevant cross sections [50] at 6 GeV/c are $\sigma(\pi^- + p \rightarrow \Lambda + K^{0*}) \simeq 10 \mu\text{b}$ and $\sigma(\pi^- + p \rightarrow \Lambda + K_s) \simeq 12 \mu\text{b}$. Again using $\frac{1}{2}$ of the peak H cross sections from Eq. (4.16), and assuming a 2% target, we obtain

$$P = \begin{cases} 1.2 \times 10^{-12} & \text{for reaction (5.2b) ,} \\ 9.8 \times 10^{-13} & \text{for reaction (5.2d) .} \end{cases}$$

Using a π^- flux at 6 GeV/c of $1.9 \times 10^9 \text{ sec}^{-1}$ at KAON, the above values of P correspond to 8 or 6.7 H event/h for (5.2b) or (5.2d), respectively. The possible enhancement of the H/d ratio by a factor 8, discussed above, has not been included here. The most favorable case would appear to be (5.2d), which involves a $K^+K^-\pi^-$ trigger, for which the background is certainly lower than for $K^+\pi^+\pi^-$. Thus, H searches with a 6 GeV/c π^- beam appear to be feasible to KAON.

At the lower pion momentum of 2.5 GeV/c, the KAON beam intensity is higher than at 6 GeV/c, and the first-stage hyperon production cross sections for (5.2a)–(5.2d) are larger. However, the second-stage H production is diminished due to threshold effects. At 2.5 GeV/c, a 0.5% rather than a 2% interaction length target is needed in order to match the shorter decay lengths of the hyperons. Using $\sigma(\pi^- + p \rightarrow \Lambda + K_s) \simeq 0.08$ mb and $\sigma(\Lambda + p \rightarrow H + K^+) \simeq 4 \mu\text{b}$, one-sixth of peak value, and a 10% detection efficiency as before, we estimate 10 counts/h for reaction (5.2b) at 2.5 GeV/c, and a very similar rate for (5.2d), comparable to the event rates given above for 6 GeV/c π^- 's.

B. Reactions with Σ^- beams at 20 GeV/c

We consider a hyperon-beam experiment, in particular, the $\Sigma^- + p \rightarrow K^{0*} + H$ reaction in the vicinity of 20 GeV/c. Information about Σ^- beams in this momentum range is known from earlier work [51] at CERN and Brookhaven. A rate of approximately 200 Σ^- and 2 Ξ^- / proton burst (1.5×10^{11} protons) was achieved in the 1970's at BNL. The limiting factor in the hyperon rate was not the proton-beam intensity, but rather the single rates expected from the background muon flux [52].

Recently, new design studies [53] have been carried out for a 20 GeV/c Σ^- beam at KAON. In this scheme, the hyperon-production target would be at the center of a sector of two circular magnets with opposite magnetic fields [54]. This has the advantage of trapping low-momentum particles such as muons. Optimistically, we estimate that a Σ^- -beam intensity of order $3 \times 10^4 \text{ sec}^{-1}$ may be attainable. This is 150 times higher than the rate obtained at BNL.

The Σ^- decay length at 20 GeV/c is 79 cm, which allows the use of a 5% interaction thickness liquid hydrogen target. Assuming $\sigma(\Sigma^- + p \rightarrow H + K^{0*}) \simeq 0.1$ nb from Eq. (4.13b), a total cross section for Σ^-p interactions of 20 mb, and a detector acceptance of 50%, we find that the probability of an interaction in a 5% interaction target is $P \simeq 1.3 \times 10^{-10}$. At a beam rate of $3 \times 10^4 \text{ sec}^{-1}$, we then expect about 1.4×10^{-2} H event/h. If a geometrical enhancement factor of 8 is included for the H , as discussed above, about 100 events would be accumulated in 1000-h run. Such an experiment is clearly very difficult.

C. Hyperon beams at high momentum (350–600 GeV/c)

Cross sections for two-body reactions [see Eq. (3.8)] become unmeasurably small at high momentum. Thus, if we wish to exploit the Σ^- beams at CERN (350 GeV/c) or Fermilab (600 GeV/c), we need to focus on inclusive or semi-inclusive reactions. In this case, it is necessary to detect the decay products of the H . The only two-body decay mode involving two charged particles is $H \rightarrow \Sigma^- p$; the $\Sigma^0 n$ or Λn decays would be very difficult to reconstruct. This if $m_H < 2.14$ GeV, all the H decay modes involve neutral particles, and a meaningful experiment is essentially impossible. If the H is a weakly bound $\Lambda\Lambda$

state, on the other hand, the H lifetime must approach $\tau_\Lambda/2 \approx 135$ ps, and the dominant decay mode becomes $H \rightarrow \Lambda N \pi$. In this case, the four-body final state $p \pi^- p \pi^-$ will be prominent and could be detected. At high momentum, the decay length is sufficiently long so that the Σ^- can be measured magnetically before it decays to a π^- and a neutron.

As part of experiment WA89 at CERN [39], which uses a 350 GeV/c Σ^- beam, and experiment E781 at Fermilab [40] (600 GeV/c), searches for the decay $H \rightarrow \Sigma^- p$ are intended. As argued in Sec. II, the H would be frequently accompanied by a \bar{p} if it is formed in a $\Xi^- + p$ collision at high energy. The Pomeron-exchange mechanism of Fig. 2 is expected to dominate. The $\Xi^- + p \rightarrow H + \bar{p} + X$ reaction is more favorable experimentally than $\Sigma^- + p \rightarrow H + \bar{\Sigma}^- + X$ because \bar{p} detection is straightforward, and the $\bar{\Sigma}^-$ cannot be distinguished from beam-related Σ^- 's. However the Ξ^- component of the Σ^- beams at CERN and Fermilab is only a few percent. The Σ^- flux is 10^5 sec^{-1} at CERN, so one expects on the order of $10^3 \Xi^-/\text{sec}$. Given the cross-section estimate $\sigma(\Xi^- + p \rightarrow H + \bar{p} + X) \sim 1 \mu\text{b}$ from Eq. (4.19), one expects a very modest rate of H events. The advantage of detecting a \bar{p} in coincidence with the decay $H \rightarrow \Sigma^- p$ is that the background would be strongly reduced. The higher energy of the Fermilab experiment is more suitable for this tagging technique. For this case, the H is produced with an energy of about 400 GeV, and the decay Σ^- has about 200 GeV, corresponding to a decay length of 7.4 m. For the CERN experiment, the final Σ^- will have roughly one-half of this decay length. The larger decay length at Fermilab is better matched to magnetic detection of the Σ^- .

VI. CONCLUSIONS AND PROSPECTS

We have presented cross-section estimates for the production of the double-strange H dibaryon in reactions induced by meson (K^-, π^\pm) or hyperon (Σ^-, Λ, Ξ^-) beams. We investigated two-body reactions of the type $Y + N \rightarrow H + M$, where the meson M is detected. The H could then be seen as a peak in the missing mass spectrum without the necessity of detecting its decay products. We also consider two-step reactions such as $M + NN \rightarrow H + M' + M''$, which take place on two nucleons. Here the first-stage process $M + N \rightarrow Y + M'$ produces a hyperon Y , which then creates the H through a second reaction $Y + N \rightarrow H + M''$. The nucleon-nucleon (NN) pair could be two protons in a liquid hydrogen target or a deuteron (d).

Our main focus is on the feasibility of experiments which could eventually be carried out at the KAON facility [49], which would offer unprecedented K^-, π^\pm , or Σ^- -beam intensities. At 6 GeV/c, fluxes of $1.5 \times 10^7 \text{ sec}^{-1}$ for K^- and $1.9 \times 10^9 \text{ sec}^{-1}$ for π^- are anticipated at KAON, which we estimate would yield 10–100 H 's in a 1000-h run with K^- 's and a factor of 100 more with π^- 's using a liquid hydrogen target. There is a substantial theoretical uncertainty in this number due to the expected strong variation of the H/d ratio with H binding energy, as well as an experimental factor depending on

the details of the detector design (we have simply assumed a 10% detection efficiency). At 6 GeV/c, such experiments appear to be feasible with π^- 's, assuming one can make use of the full beam intensity. At a lower momentum of 2.5 GeV/c, an even higher π^- flux of order $1.6 \times 10^{10} \text{ sec}^{-1}$ could be available. However, the cross section for production of two units of strangeness drops rapidly as we descend to these lower momenta, and we estimate comparable counting rates for H production with 2.5 and 6 GeV/c π^- beams. For these reactions, we detect three charged mesons in the final state ($K^0 K^+ \rightarrow \pi^+ \pi^- K^+$ or $K^{0*} K^+ \rightarrow \pi^- K^+ K^+$).

For a hypothetical Σ^- hyperon beam at KAON, at 20 GeV/c with an intensity of $3 \times 10^4 \text{ sec}^{-1}$ we expect 10–100 H 's to be produced in a 1000-h run, assuming an input cross section $\sigma(\Sigma^- + p \rightarrow H + K^{0*}) \approx 0.1 \text{ nb}$. In this case, we detect the decay products $K^+ \pi^-$ of the K^{0*} . Such an experiment appears to be marginal for KAON. The cross section for H production with a Ξ^- is larger than that for a Σ^- , but the Ξ^- component of the Σ^- beam at KAON would only constitute 1% or so, and thus only a few additional H 's would be produced.

We have also considered the use of existing high-momentum Σ^- beams at CERN (350 GeV/c) or Fermilab (600 GeV/c) to produce the H . In experiment WA89 at CERN [39], and E781 at Fermilab [40], the decay $H \rightarrow \Sigma^- p$ will be searched for. Two-body cross sections at high momenta are hopelessly small, so one must investigate inclusive or semi-inclusive processes, and detection of the H decay products is obligatory. We suggest that for $\Xi^- + p$ reactions at high energy, the H may be often accompanied by a \bar{p} . The simultaneous detection of the \bar{p} and the decay $H \rightarrow \Sigma^- p$ may serve to significantly improve the signal/background ratio.

Finally, we mention that the Pomeron-exchange mechanism (Fig. 2) also offers the possibility of producing the \bar{H} (antiparticle of the H) as well as the pentaquark P , a proposed [4,5] isospin $I = \frac{1}{2}$ doublet ($P^0 = \bar{c}uuds$, $P^- = \bar{c}ddus$). Some of the relevant reactions are

$$\begin{aligned} \bar{p} + p &\rightarrow \bar{H} + \Xi^- + X, \\ \bar{p} + p &\rightarrow \bar{P}^0 + D_s^- + X, \\ p + p &\rightarrow P^0 + D_s^+ + X, \\ \Sigma^+ + p &\rightarrow P^0 + D^+ + X, \\ \Sigma^- + p &\rightarrow P^- + D^0 + X, \end{aligned}$$

where $D_s^-(\bar{c}s)$, $D_s^+(c\bar{s})$, $D^+(c\bar{d})$, and $D^0(c\bar{u})$ are charmed mesons. The pentaquark cross sections depend on the charm-anticharm meson ($D_s^- D_s^+$, $D^- D^+$, $D^0 D^0$) components in the Pomeron, about which very little is known. However, the detection of a D meson would provide an important experimental tag of P formation. If the P is stable with respect to strong decays ($P^0 \rightarrow p D_s^-$, for instance), one would try to reconstruct a weak decay involving only charged particles, for example, $P^0 \rightarrow p \phi \pi^-$.

ACKNOWLEDGMENTS

This work was supported under Contract No. DE-AC02-76CH00016 with the U.S. Department of Energy and by the U.S.-Israel Binational Science Foundation (BSF), Jerusalem, Israel. We would like to thank D.

Ashery, B. Basselleck, P. Cooper, and A. Gal for useful discussions, and I. Strakovsky for providing a compilation of deuteron-production references. H. J. L. would like to thank the Nuclear Theory Group for their hospitality during a visit to Brookhaven as part of the 1991 summer program.

-
- [1] R. L. Jaffe, Phys. Rev. Lett. **38**, 195 (1977); **38**, 1617(E) (1977).
- [2] P. J. Mulders, A. T. Aerts, and J. J. deSwart, Phys. Rev. D **21**, 2653 (1980).
- [3] J. L. Rosner, Phys. Rev. D **33**, 2043 (1986).
- [4] H. J. Lipkin, Phys. Lett. B **195**, 484 (1987); Nucl. Phys. **A478**, 307c (1988).
- [5] C. Gignoux, B. Silvestre-Brac, and J. M. Richard, Phys. Lett. B **193**, 323 (1987).
- [6] A. P. Balachandran, F. Lizzi, V. G. J. Rodgers, and A. Stern, Nucl. Phys. **B256**, 525 (1985).
- [7] R. L. Jaffe and L. I. Korpa, Nucl. Phys. **B258**, 468 (1985).
- [8] C. G. Callen and I. Klebanov, Nucl. Phys. **B262**, 365 (1985).
- [9] M. Oka, K. Shimizu, and K. Yazaki, Phys. Lett. **130B**, 365 (1983).
- [10] U. Straub, Zong-Ye Zhang, K. Bräuer, A. Faessler, and S. B. Khadkikar, Phys. Lett. B **200**, 241 (1988).
- [11] K. Nishikawa, N. Aoki, and H. Hyuga, Nucl. Phys. **A534**, 573 (1991).
- [12] M. Oka and S. Takeuchi, Nucl. Phys. **A524**, 649 (1991).
- [13] Y. Iwasaki, T. Yoshie, and Y. Tsuboi, Phys. Rev. Lett. **60**, 1371 (1988).
- [14] P. MacKenzie and H. Thacker, Phys. Rev. Lett. **55**, 2359 (1985).
- [15] J. F. Donoghue, E. Golowich, and B. R. Holstein, Phys. Rev. D **34**, 3434 (1986).
- [16] C. B. Dover, D. J. Millener, A. Gal, and D. H. Davis, Phys. Rev. C **44**, 1905 (1991).
- [17] M. Oka, K. Shimizu, and K. Yazaki, Nucl. Phys. **A464**, 700 (1987); Y. Koike, K. Shimizu, and K. Yazaki, *ibid.* **A513**, 653 (1990).
- [18] M. Bozoian, J. C. H. van Doremalen, and H. J. Weber, Phys. Lett. **122B**, 138 (1983).
- [19] B. A. Shahbazian, A. O. Kechechyan, A. M. Tarasov, and A. S. Martynov, Z. Phys. C **39**, 151 (1988).
- [20] G. B. Franklin, Nucl. Phys. **A450**, 117c (1986).
- [21] P. Barnes, in *Proceedings of the International Symposium on Hypernuclear and Low-Energy Kaon Physics*, Padua, 1988, edited by T. Bressani *et al.* (Societa Italiana de Fisica); Nuovo Cimento A **102**, 541 (1989).
- [22] A. T. M. Aerts and C. B. Dover, Phys. Rev. D **29**, 433 (1984).
- [23] K. Kilian, in *Physics at LEAR with Low Energy Antiprotons*, Fourth Lear Workshop, Villars-sur-Ollon, Switzerland, edited by C. Amsler *et al.*, Nuclear Science Research Conference Series Vol. 14 (Harwood, Academic, Chur, Switzerland, 1987), p. 529.
- [24] C. B. Dover, P. Koch, and M. May, Phys. Rev. C **40**, 115 (1989).
- [25] C. B. Dover, U. Heinz, E. Schnedermann, and J. Zimanyi, Phys. Rev. C **44**, 1636 (1991).
- [26] J. Sandweiss, R. Majka *et al.*, BNL proposal E864, 1990 (unpublished).
- [27] Tsu Yao, Phys. Rev. **134**, B454 (1964).
- [28] D. J. Brown, Nucl. Phys. **B7**, 37 (1968).
- [29] D. J. Brown and M. K. Sundaresan, Nuovo Cimento A **55**, 346 (1968).
- [30] V. Barger and C. Michael, Phys. Rev. Lett. **22**, 1330 (1969).
- [31] We are indebted to Frank Paige for illuminating discussions on high-energy production mechanisms.
- [32] A. Donnachie and P. V. Landshoff, Nucl. Phys. **B244**, 322 (1984); **B267**, 690 (1986).
- [33] H. L. Anderson *et al.*, Phys. Rev. Lett. **21**, 853 (1968).
- [34] W. F. Baker *et al.*, Phys. Rev. **136**, B779 (1964).
- [35] J. V. Allaby *et al.*, Phys. Lett. **29B**, 198 (1969).
- [36] U. Amaldi *et al.*, Lett. Nuovo Cimento **4**, 121 (1972).
- [37] D. R. O. Morrison, Phys. Lett. **22**, 528 (1966).
- [38] L. Csernai and J. Kapusta, Phys. Rep. **131**, 223 (1986).
- [39] A. Forino *et al.*, CERN Report No. ISSN 0259-093X, p. 47, 1990 (unpublished).
- [40] J. Russ, private communication.
- [41] M. Harvey, Nucl. Phys. **A352**, 301 (1981); R. P. Bickerstaff and B. G. Wybourne, J. Phys. G **7**, 275 (1981).
- [42] M. M. Nagels, T. A. Rijken, and J. J. deSwart, Phys. Rev. D **12**, 744 (1975); **15**, 2547 (1977); **20**, 1633 (1979).
- [43] E. Hirsch, U. Karshon, and H. J. Lipkin, Phys. Lett. **36B**, 385 (1971).
- [44] P. Baillon *et al.* Phys. Lett. **50B**, 383 (1974); Nucl. Phys. **B134**, 31 (1978).
- [45] J. Bailly *et al.*, Phys. Lett. B **195**, 609 (1987).
- [46] J. Bystricky *et al.*, J. Phys. (Paris) **48**, 1901 (1987).
- [47] V. Fitch, in *Proceedings of the 10th Hawaii Conference in High Energy Physics* (University of Hawaii Press, 1985).
- [48] C. B. Dover, Nucl. Phys. **A450**, 95c (1986).
- [49] TRIUMF report 1985 (unpublished); The anticipated beam intensities at 6 GeV/c given in the text are for the K6 beam line, while those at 2.5 GeV/c refer to the K2.5 line (E. Vogt, private communication).
- [50] V. Flaminio *et al.*, CERN Report No. 79-02, 1979 (unpublished).
- [51] Charged-hyperon beams are described in several review articles: J. Lack and L. Pondrom, Annu. Rev. Nucl. Part. Sci. **29**, 203 (1979); M. Bourquin and J. P. Repellin, Phys. Rep. **114**, 100 (1984); J. M. Gaillard and G. Savage, Annu. Rev. Nucl. Part. Sci. **34**, 351 (1984); L. Pondrom, Phys. Rep. **122**, 57 (1985).
- [52] W. Tanenbaum *et al.* Phys. Rev. D **12**, 1871 (1975).
- [53] C. Wiedner, in *Proceedings of the KAON Workshop*, Vancouver, 1990 (unpublished).
- [54] C. Tschalaer, Nucl. Instrum. Methods A **249**, 171 (1986).